

## REACTION ZONE STRUCTURE IN FLAMELESS COMBUSTION

KAORU MARUTA,<sup>1</sup> KATSUTOSHI MUSO,<sup>2</sup> KOICHI TAKEDA<sup>1</sup> AND TAKASHI NIIOKA<sup>2</sup>

<sup>1</sup>*Faculty of Systems Science and Technology*

*Akita Prefectural University*

*84-4 Tsuchiya-Ebinokuchi, Honjyo, Akita 015-0055, Japan*

<sup>2</sup>*Institute of Fluid Science*

*Tohoku University*

*2-1-1 Katahira, Aoba, Sendai 980-8577, Japan*

We present a study of the combustion limit and reaction zone structure of non-premixed counterflow flames of highly preheated air and methane diluted with nitrogen.

First, we measured the flammable region experimentally in the range of air temperatures up to 800 K. In the case of flame stretch rates smaller than  $20 \text{ s}^{-1}$ , experiments were conducted under microgravity. All the microgravity tests were conducted at the JAMIC drop tower facility in Hokkaido, Japan. The results show that the extinction limits become broader with increasing air temperature. All the extinction curves are C-shaped and exhibit the radiation extinction branch. That is, the configurations of the extinction curves are the same as those of conventional combustion at air temperatures from 300 K to 800 K.

Second, we computed the flammable region and reaction zone structure of these flames by using the conventional one dimensional flame code with detailed chemistry. The flammable regions obtained by experiment agree with the computated ones. This shows that the present computation could also represent the phenomena well for high-temperature air combustion. Based on this, computation was extended to higher air temperatures (up to 1900 K) at which microgravity experimentation is not possible.

When the air temperature was higher than 1300 K, extinction limits disappeared. In this temperature range, combustion continues even under extremely fuel-lean conditions such as 1% methane in nitrogen. Reaction zones without any temperature peaks were observed. Methane and oxygen leakage through the flame occurred, and they coexisted there. This is like the Liñán's premixed flame regime, in other words, a reaction-time-dominated reaction zone structure. In these regions,  $\text{NO}_x$  emission is very low, and this may lead to the low levels of  $\text{NO}_x$  emission of high-temperature air combustion.

### Introduction

So-called high-temperature air combustion [1,2] is the combination of highly preheated air and exhaust gas recirculation that provides high thermal efficiency and low  $\text{NO}_x$  emission in practical furnaces. Pressing, Peters, and Wuenning [3] have shown the temperature uniformity and weak reaction of this combustion mode by means of laser optical measurements and have called this phenomenon *flameless combustion*. To adopt this new combustion technology for wider practical use, much more fundamental knowledge on high-temperature air combustion is needed.

Hasegawa et al. [4], Katsuki and Ebisui [5], and Sato [6] demonstrated the characteristics of high-temperature air combustion, such as low luminosity, a uniform temperature field, low levels of temperature fluctuation, low pollutant emissions, and high efficiency. Ju [7] clarified the  $\text{NO}_x$  formation mechanism of the high-temperature air combustion up to 1300 K by using a counterflow non-premixed flame configuration. Fujimori et al. [8] examined

the relation between the lift-off height of a turbulent jet flame and  $\text{NO}_x$  reduction and showed that a highly lifted flame is the key to a drastic decrease in the emission index of  $\text{NO}_x$  in high-temperature air combustion. They also suggested that the formation of the lean mixture due to the flame lift might contribute to the lower  $\text{NO}_x$  level. Ishiguro et al. [9] also confirmed the homogeneity and stability of high-temperature air combustion experimentally.

As clearly mentioned in the literature [3], this combustion mode in furnaces is established only by lifted-jet geometry. This makes laminar-flame-based fundamental research difficult and has resulted in very limited quantitative knowledge concerning this new combustion technology.

As pointed out by Fujimori et al. [8], a high-speed lifted jet flame is indispensable for establishing the low  $\text{NO}_x$  emission. This may be because the lifted jet flame suppresses the formation of a thin, intense reaction zone. The lifted flame improves the dilution of the combustible mixture that leads to slow reaction and temperature uniformity.

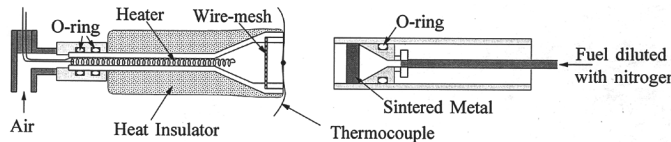


FIG. 1. Structure of the burner with an electric heater.

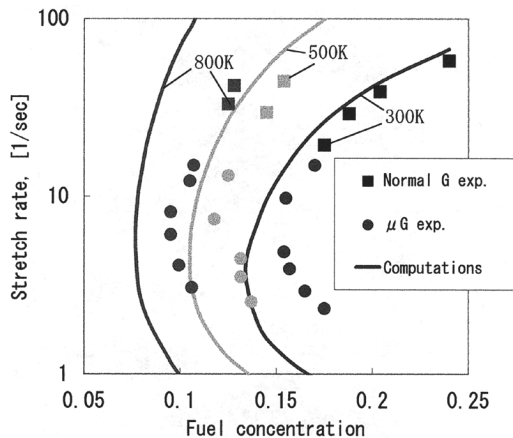


FIG. 2. Extinction curve obtained under microgravity.

To resolve these processes and to understand high-temperature air combustion further, laminar-flame-based fundamental research on high-temperature air combustion is needed. In addition to that, because the flow field inside the furnace is not always highly turbulent, high-temperature air combustion in low-speed and low-strained flow fields should be clarified to reproduce the excellent emission characteristics.

For all these reasons, a combination of microgravity experiment and computation with detailed chemistry on low-stretch, counterflow, non-premixed flames was employed. Because the low-stretch counterflow flame technique under microgravity [10] is one of the best methods to observe combustion limits and to examine characteristics of near-limit combustion experimentally, we have tried to clarify the extinction limit, combustion characteristics, and reaction zone structure of high-temperature air combustion, especially in the fuel-lean region.

### Microgravity Experiments

Because the details of the experimental setup have been described elsewhere [10], only an outline is given here. The system consisted of a counterflow pipe burner (16 mm in diameter), electric mass flow controllers, a notebook PC, digital/analogue and analogue/digital converters, a thermocouple for recording gas temperature at the burner exit, air and fuel containers, and a video system. The flow rate of

the gas mixture was previously programmed and controlled by the digital/analogue converter and flow controller. One side of the burner had an electric heater to heat the air, as shown in Fig. 1. To obtain sufficient heat exchange between heater and air flow, the inner diameter of the heater part was thinner than the burner exit. To minimize heat loss from this burner, the burner body was covered with a heat insulator. Stable airflow with temperatures higher than 800 K was obtained with the present burner. The air temperature was regulated to within 5°.

Counterflow flames of air, whose temperature ranged from 300 K to 800 K, and methane diluted with nitrogen were employed for the present investigation. For flame stretch rates below  $20 \text{ s}^{-1}$ , microgravity experiments were conducted at the JAMIC drop tower facility in Hokkaido, Japan. Ten seconds of microgravity during 490 m free-fall is available in this facility. Because of the difficulty of velocity measurement under microgravity, stretch rate was estimated by the nominal value given by Seshadri and Williams [11].

### Computation

One-dimensional computation with detailed chemistry covered a wider air temperature range than did the experimental conditions. The numerical codes used [12,13] were based on the work by Giovangigli and Smooke [14]. An optically thin radiative heat loss from  $\text{CO}_2$  and  $\text{H}_2\text{O}$  was taken into account because it would not be negligible at small stretch rates [10,12,15]. The CHEMKIN [16] code and an appropriate chemical mechanism were chosen. For the calculation of extinction limits, a  $\text{C}_1$  elementary reaction mechanism [14] which involves 58 reactions and 18 species was used. For the calculation of the  $\text{NO}_x$  emission, GRI-Mech 2.11, whose validity for combustion in high-temperature air was confirmed by experiment [17], was employed.

### Results and Discussion

#### Microgravity Experiments

Figure 2 shows extinction curves obtained in the microgravity experiments. For air temperatures of 300 K to 800 K, C-shaped extinction curves with a radiation extinction branch were observed. Flammable regions were extended with increase in the air

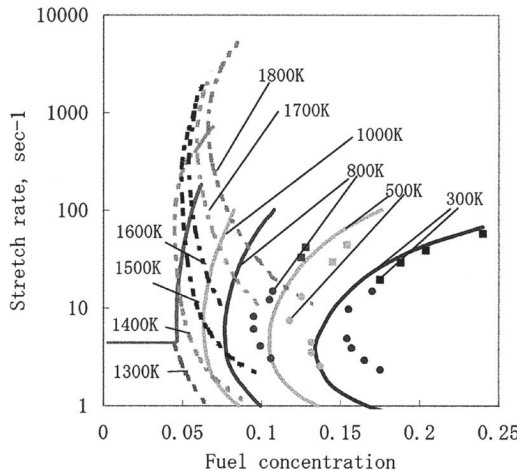


FIG. 3. Extinction curve obtained by computation with  $C_1$  chemistry.

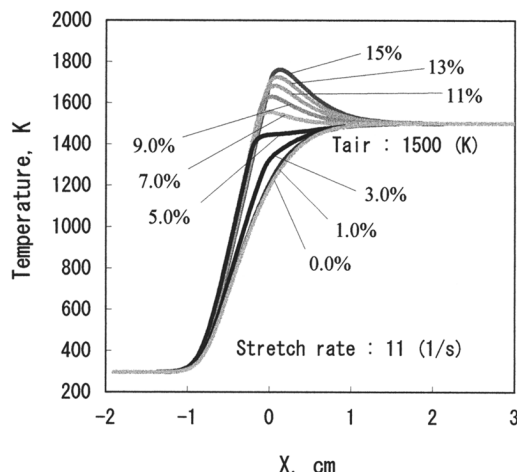


FIG. 4. Temperature profile along the  $x$  axis at an initial air temperature of 1500 K.

temperature. The result for an air temperature of 300 K was identical to the data reported previously [15]. For comparison, the computational results as well as the experimental ones are indicated in the same figure. Both sets of results agree qualitatively with each other, confirming the validity of the present computation.

#### Computational Results

Extinction curves obtained by computation are shown in Fig. 3. The range of preheated air temperature has been widened to 1800 K. Extinction curves for air temperatures higher than 800 K are

available only by calculation because of experimental limitations. The dotted lines do not denote extinction limits but rather the points where the preheated air temperature and peak of the reaction zone temperature become equal. When the air temperature is higher than 1300 K, extinction limits disappear because the preheated air carries enough energy into the reaction region. The general trend of the extinction characteristics was the same as that for the air temperature of 300 K as far as the combustion limit existed.

To explain the disappearance of the extinction limit, the temperature distribution along the axis is shown in Fig. 4. This figure shows the temperature distribution when the air temperature is 1500 K and the stretch rate is  $11 \text{ s}^{-1}$ . The methane mole fraction of the fuel flow,  $C_{\text{fuel}}$ , is varied as a parameter. When  $C_{\text{fuel}}$  is larger than 7%, a temperature peak due to the exothermic reaction can be observed. However, the temperature peak reduces with the decrease of  $C_{\text{fuel}}$  and cannot be seen when  $C_{\text{fuel}}$  is smaller than 5%. However, a moderate chemical reaction is going on for those conditions. Other intermediate species concentration distribution, such as of  $\text{CH}$ ,  $\text{CO}$ , and  $\text{H}$ , proved the continuation of the reaction, although they are not shown here. Fuel concentrations at the disappearance of the temperature peak are shown as dotted lines in Fig. 3. Combustion of counterflow non-premixed flames of highly preheated air in the fuel-lean region is characterized by this disappearance of extinction limits and chemical reaction without an obvious temperature rise.

In considering the nature of a flame without a temperature peak, which we call *flameless combustion*, we follow Pressing et al., who also used this term for combustion in highly preheated air [3]. To answer the question of why the reaction proceeds, we consider a peculiarity of high-temperature air combustion. In conventional combustion, some of the loss mechanism is responsible for the existence of combustion limits. For instance, conduction heat loss to the wall, flame stretch, and radiation heat loss are the reasons why combustion limits always exist. However, it always depends on the balance between heat generation and heat loss. High-temperature air combustion is a kind of excess enthalpy combustion [18]. Because of this, the balance needed for extinction could not be established in a situation like that indicated in Fig. 4.

When the fuel entering the reaction zone is decreased in the fuel-lean regime the heat release rate due to reaction might be further decreased. To quantify this, the dependence of the total heat release rate on  $C_{\text{fuel}}$  at the same air temperature and the stretch rate is plotted as shown in Fig. 5. The total heat release rate is defined as  $\int \sum_k h_k \cdot \dot{\omega}_k dX$ , where  $h_k$  and  $\dot{\omega}_k$  are the enthalpy of the  $k$ th species and the production rate of the  $k$ th species, respectively. The total heat release rate decreases with decreasing  $C_{\text{fuel}}$ . Especially when  $C_{\text{fuel}}$  is smaller than

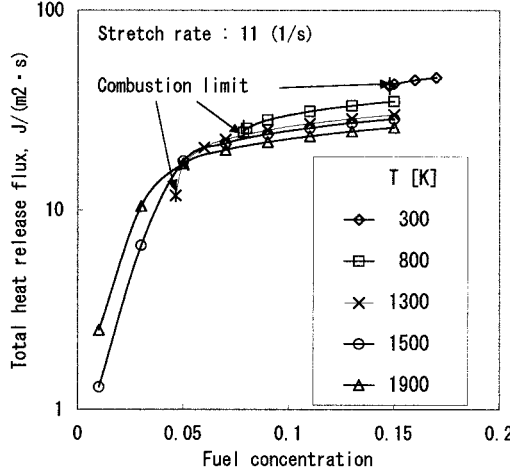


FIG. 5. Variation of total heat release rate with fuel concentration.

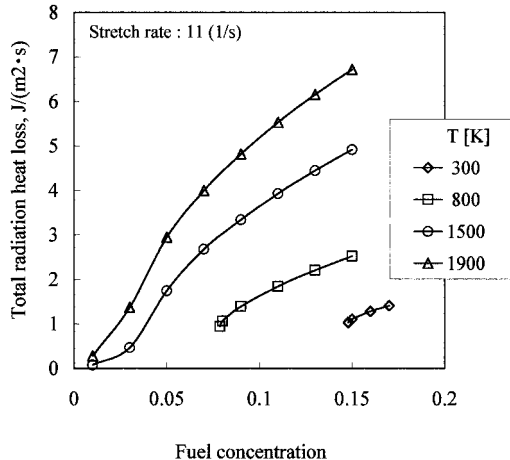


FIG. 6. Variation of the total radiation heat loss with fuel concentration.

5%, the gradient of the decrease of the total heat release rate becomes steeper. This tendency implies the temperature distribution shown in Fig. 4.

Because radiation heat loss often dominates the flame characteristics close to the combustion limit, total radiation heat loss from the reaction zone was plotted in Fig. 6 to examine the characteristics shown in Fig. 4. However, since the stretch rate is constant, the total amount of the radiation heat loss mostly depends on the heat generation in this case. The total radiation heat loss decreases with decreasing fuel concentration,  $C_{fuel}$ , which shows that the radiation heat loss is not the relevant mechanism of the trend shown in Fig. 4. The radiation fraction [12] defined by the ratio of the total radiation loss to the

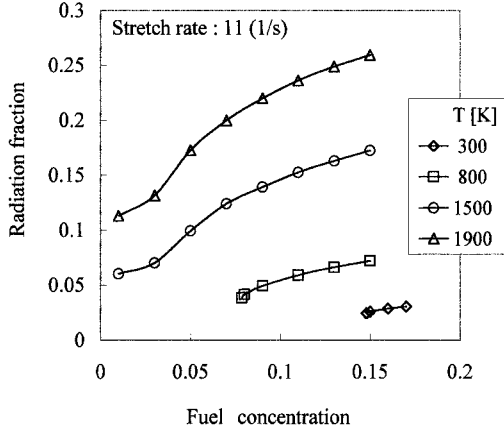


FIG. 7. Variation of radiation fraction with fuel concentration.

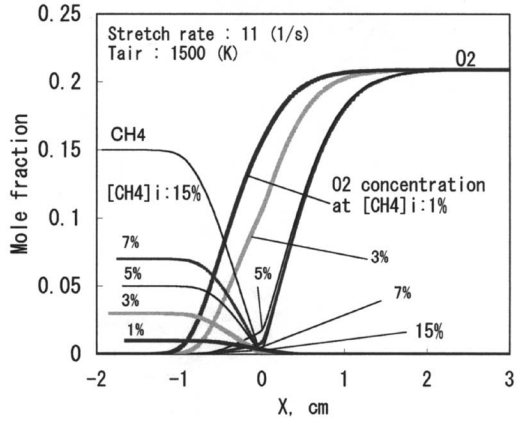


FIG. 8. Profiles of methane and oxygen mole fractions along the x axis.

total heat release rate is shown in Fig. 7. The radiation fraction also decreases with the fuel concentration,  $C_{fuel}$ , because the stretch rate is kept constant, which shows that the radiation loss does not dominate the low heat release rate in the fuel-lean region.

To examine the moderate reaction region observed when  $C_{fuel}$  is smaller than 5%, the concentration distribution of major species such as methane and oxygen are shown in Fig. 8. As is clearly shown in the figure, the thin flamelet assumption stands only when  $C_{fuel}$  is greater than 5%, that is, methane and oxygen are consumed at the thin flame region and the reaction rate can be regarded as sufficiently high. However, oxygen and methane concentration distributions cross over when  $C_{fuel}$  is less than 5%. This region is similar to the so-called Liñán's premixed flame regime [19]. Although Liñán's premixed

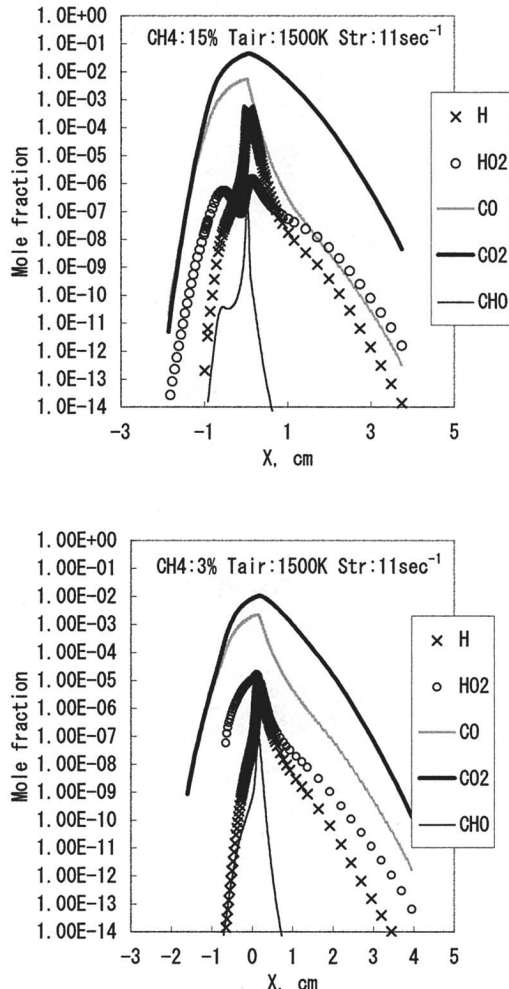


FIG. 9. Profiles of CO, CO<sub>2</sub>, H, HO<sub>2</sub>, and CHO mole fractions along the  $x$  axis.

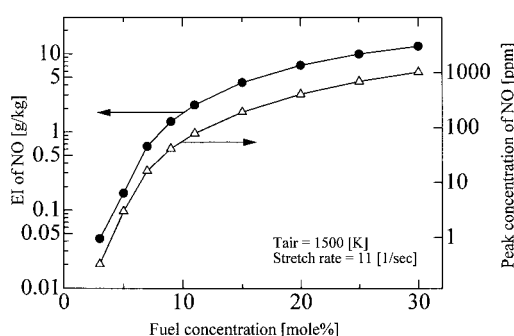


FIG. 10. Emission index and peak concentration of NO.

flame regime is approached only close to the combustion limit, the present fuel and oxygen leakage never led to extinction, since the energy that high-temperature air brings into the reaction zone is high enough to sustain a weak reaction.

From discussion based on timescales such as the reaction and residence times, this premixed flame-like regime appears at very fuel-lean conditions where the reaction time is larger than the residence time. Hence this can be regarded as a reaction-controlled phenomenon. The timescale of this condition is around 100 ms, so the present reaction time is larger than this value. One previous study [3] clearly states that “the highly preheated air combustion is mixing controlled,” and another [8] notes that “pre-mixture properties of fuel, air and also pyrolysis fuel gas may affect the emission characteristics of high-temperature air combustion,” which implicitly suggests that it is a reaction-controlled system. The present premixed flame regime may be somewhat relevant to the mechanism of high-temperature air combustion.

For comparison of the fuel concentrations of  $C_{\text{fuel}}$  for 15% and 3%, chemical species concentrations such as CO<sub>2</sub>, CO, H, CHO, and HO<sub>2</sub> are shown in Fig. 9. CO and CO<sub>2</sub> concentrations in those two cases do not differ greatly from each other. However, the peak concentration of H for  $C_{\text{fuel}}$  of 15% is 1 order of magnitude larger than that at  $C_{\text{fuel}}$  of 3%. In addition to this, the configurations of the HO<sub>2</sub> distributions are quite different from each other. When  $C_{\text{fuel}}$  is 15%, it has two peaks, but when it is 3%, it has only one peak. This suggests that there might be some differences in chemical reaction for these two cases.  $\text{H} + \text{O}_2 + \text{M} \rightarrow \text{HO}_2 + \text{M}$  might play some role in this, because the peak concentration of HO<sub>2</sub> at  $C_{\text{fuel}}$  3% is 10 times larger than that at  $C_{\text{fuel}}$  15%, while the peak concentration of H has the opposite tendency.

The NO<sub>x</sub> emission characteristics of these flames were examined by using GRI-Mech 2.11 for the same conditions as for the above computation. The results of temperature and major species distribution were confirmed to be almost the same as those obtained by using C<sub>1</sub> chemistry. Fig. 10 shows the emission index of NO and its peak concentration along the axis. Because the concentrations of the NO<sub>2</sub> and N<sub>2</sub>O are at least 2 orders of magnitude smaller than that of NO, the present NO emission index could be a measure of the total NO<sub>x</sub> emission index of the present combustion system. As shown in the figure, the emission index of NO and its peak concentration have the almost same trend with the fuel concentration. Both decrease with decreasing fuel concentration, and the emission level of NO was very low especially in the smaller fuel concentration region. However, no significant changes of emission characteristics were observed at the boundary of the thin flamelet region and reaction-controlled flame

region discussed above. Although much of the oxygen coexists with the fuel in the reaction-controlled region, the thermal mechanism might not be so active because of the low temperature. A discussion of the mechanism of NO formation in high-temperature air combustion appears in Ref. [7].

In this study, low oxygen concentration that might be the model for exhaust gas recirculation is not computed. Although the relation between the present flameless combustion and the so-called high-temperature air combustion remains unclear, we have shown that low fuel concentration and high temperature air exhibit the favorable characteristics of high-temperature air combustion using atmospheric air.

In furnaces operated under conditions of high-temperature air combustion, heat transfer to the load to be heated is better than for conventional combustion. One reason for this characteristic might be the effect of radiation heat transfer. Another effect may be the uniform temperature distribution. The existence of a weak reaction zone may play some role in the uniform temperature distribution.

Yoshida et al. [20] described flame structure and emission characteristics in a jet-stirred reactor. They used a highly preheated inlet air jet and strong exhaust gas recirculation in the intensely turbulent zone. The nature of the combustion field is very similar to that of flameless combustion in the furnace, except for the high turbulence level. They found several specific characteristics in the jet-stirred reactor such as the coexistence of fuel and oxygen, and extremely low levels of  $\text{NO}_x$  emission. The emission index of  $\text{NO}_x$  ranged from 0.01 to 0.5 g/(kg-fuel). These two combustion characteristics are exactly the same as those of the present counterflow flameless combustion in the laminar flow field, perhaps because of its very slow reaction time.

## Conclusions

Microgravity experiments and computation employing detailed chemistry were carried out to examine the combustion characteristics and reaction zone structure of high-temperature air combustion in a counterflow non-premixed flame. The main results are as follows:

1. Radiation extinction occurred and C-shaped extinction curves were obtained at air temperatures of 300 K, 500 K, and 800 K.
2. At air temperatures higher than 1300 K, the extinction limit disappeared because of the high energy that the high-temperature air carried into the reaction zone.
3. Moderate reaction without any temperature peak was observed under fuel-lean conditions where the NO emission is very low.

## Acknowledgments

The authors thank Profs. Hideaki Kobayashi and Yiguang Ju of Tohoku University for their stimulating discussions, and Mr. Susumu Hasegawa for his assistance with the microgravity experiments. This work was performed under the management of the Japan Space Utilization Promotion Center as a part of an R&D project on advanced furnaces and boilers supported by the New Energy and Industrial Technology Development Organization.

## REFERENCES

1. Katsuki, M., and Hasegawa, T., *Proc. Combust. Inst.* 27:3135–3146 (1998).
2. Niioka, T., *Proceedings of the Fifth ASME/JSME Joint Thermal Engineering Conference*, San Diego, CA, 1999, pp. 1–6.
3. Pressing, T., Peters, N., and Wuenning, J. G., *Proc. Combust. Inst.* 27:3197–3204 (1998).
4. Hasegawa, T., Tanaka, R., and Niioka, T., in *Proceedings of the International Joint Power Generation Conference EC-Vol. 5*, Book No. G017072, (Sanyai et al., eds.), ASME International, 1997, pp. 259–266.
5. Katsuki, M., and Ebisui, K., in *First Asia-Pacific Conference on Combustion*, The Australia/New Zealand, Chinese, Chinese Taipei, Japanese and Korean Sections of the Combustion Institute, 1997, pp. 294–297.
6. Sato, J., in *First Asia-Pacific Conference on Combustion*, The Australia/New Zealand, Chinese, Chinese Taipei, Japanese and Korean Sections of the Combustion Institute, 1997, pp. 286–289.
7. Ju, Y., in *First Asia-Pacific Conference on Combustion*, The Australia/New Zealand, Chinese, Chinese Taipei, Japanese and Korean Sections of the Combustion Institute, 1997, pp. 460–463.
8. Fujimori, T., Riechelmann, D., and Sato, J., *Proc. Combust. Inst.* 27:1149–1155 (1998).
9. Ishiguro, T., et al., *Proc. Combust. Inst.* 27:3205–3213 (1998).
10. Maruta, K., Yoshida, M., Ju, Y., and Niioka, T., *Proc. Combust. Inst.* 26:1283–1289 (1996).
11. Seshadri, K., and Williams, F. A., *Int. J. Heat Mass Transfer* 21:251–253 (1978).
12. Guo, H., Ju, Y., Maruta, K., Niioka, T., and Liu, F., *Combust. Flame* 109:639–646 (1997).
13. Ju, Y., Guo, H., Maruta, K., and Liu, F., *J. Fluid Mech.* 342:315–334 (1997).
14. Giovangigli, V., and Smooke, M. D., *Combust. Sci. Technol.* 53:23–49 (1987).
15. Maruta, K., Yoshida, M., Guo, H., Ju, Y., and Niioka, T., *Combust. Flame* 112:181–187 (1998).
16. Kee, R. J., Grcar, J. F., Smooke, M. D., and Miller, J. A., Sandia report SAND85-8240, 1994.
17. Fuse, R., Kobayashi, H., Ju, Y., Maruta, K., and Niioka, T., *Thirty-Seventh Symposium (Japanese) on Combustion*, Japanese section of the Combustion Institute, 1999, pp. 459–460.

18. Hardisty, D. R., and Weinberg, F. J., *Combust. Sci. Technol.* 8:201–214 (1974).
19. Liñán, A., *Acta Astronaut.* 1:1007–1039 (1974).
20. Yoshida, A., Naito, H., and Narisawa, M., *Thirty-Seventh Symposium (Japanese) on Combustion*, Japanese section of the Combustion Institute, 1999, pp. 11–12.

## COMMENTS

*Bassam Dally, University of Adelaide, Australia.*

1. In furnace-type applications, where this combustion regime is most prominent, the initiation process plays an important role. Have you considered mixing your oxidant stream with combustion products?
2. You used the GRI mechanism in your calculations. How applicable is this mechanism to temperatures below 1400 K?

*Author's Reply.*

1. Yes. In fact, mixing oxidant with combustion products is one of the key processes for the high-temperature air combustion mode. But note that the present research tries to examine the sole effect of air preheating on fundamental aspects of non-premixed combustion. The results showed the appearance of a reaction-controlled regime without mixing of combustion products. To examine the effects of combustion products, treatment of radiation reabsorption that is strongly dependent on the system characteristic scale remains.
2. Our ground-based species measurements [1] on the same configuration showed that this mechanism has well predicted the measured data. From this, we conclude it can be applicable down to this temperature range.

[1] Submitted to *Combustion and Flame*.

extinction limits, discussion without considering radiative heat loss on the near-limit flame does not make sense. For this reason, microgravity conditions are indispensable.

## REFERENCE

1. Maruta, K., Yoshida, A., Guo, H., Ju, Y., and Nioka, T., *Combust. Flame* 112:181 (1998).

*Bradley Williams, Naval Research Laboratory, USA.* Does the long residence time for your flame conditions preclude the formation of superequilibrium concentrations of the major flame radical species (H, O, and OH)? If so, what effect does this have on the flame chemistry, particularly NO<sub>x</sub> formation?

*Author's Reply.* Our recent NO<sub>x</sub> measurements showed that the present modeling well predicted NO<sub>x</sub> formation for non-premixed flames in highly preheated air and fuel diluted with nitrogen. It might have an effect, but it seems not to be significant.

*Roman Weber, International Flame Research Foundation, The Netherlands.* What have you gained by conducting your experiments in microgravity?

*Author's Reply.* As shown by our previous work [1], only microgravity experiments could show the existence of radiative extinction. Under the effects of gravity, you could not extract this flame nature because of the disturbance due to the effect of buoyancy. For examining flame characteristics near their limits, such as the disappearance of

*Anthony Hamins, NIST, USA.* The very careful experiments and calculations show that the turning point strain rate is nearly invariant with air preheating. Does this suggest that the radiant fraction at the turning point is invariant for this system?

*Author's Reply.* The turning point strain rates slightly increased with the increase of the preheated air temperatures. This might be the result of the balance between (1) the incoming flow carrying larger enthalpy to the system for higher air temperature, and (2) lower fuel concentration leading to a lower amount of the radiating species.